


## RESEARCH

## Open Access



# Non-invasive absolute measurement of leaf water content using terahertz quantum cascade lasers

Lorenzo Baldacci<sup>1†</sup>, Mario Pagano<sup>2\*†</sup> , Luca Masini<sup>1</sup>, Alessandra Toncelli<sup>4</sup>, Giorgio Carelli<sup>3</sup>, Paolo Storchi<sup>2</sup> and Alessandro Tredicucci<sup>4</sup>

## Abstract

**Background:** Plant water resource management is one of the main future challenges to fight recent climatic changes. The knowledge of the plant water content could be indispensable for water saving strategies. Terahertz spectroscopic techniques are particularly promising as a non-invasive tool for measuring leaf water content, thanks to the high predominance of the water contribution to the total leaf absorption. Terahertz quantum cascade lasers (THz QCL) are one of the most successful sources of THz radiation.

**Results:** Here we present a new method which improves the precision of THz techniques by combining a transmission measurement performed using a THz QCL source, with simple pictures of leaves taken by an optical camera. As a proof of principle, we performed transmission measurements on six plants of *Vitis vinifera* L. (cv "Colorino"). We found a linear law which relates the leaf water mass to the product between the leaf optical depth in the THz and the projected area. Results are in optimal agreement with the proposed law, which reproduces the experimental data with 95% accuracy.

**Conclusions:** This method may overcome the issues related to intra-variety heterogeneities and retrieve the leaf water mass in a fast, simple, and non-invasive way. In the future this technique could highlight different behaviours in preserving the water status during drought stress.

**Keywords:** Terahertz quantum cascade laser, Water content, Drought stress, *Vitis vinifera* L.

## Background

There is an increasing need to improve the knowledge of the water resources of plant varieties, owing to the variable rainfall after climate change, in order to assess the need for irrigation [1]. In this perspective, leaves are essential organs for the water balance [2]. Leaf morphology comes from a long evolutionary process of a polyhedral anatomical structure in which the veins are definitely at the heart of this organic evolution [3]. This structure is an essential tool for the mechanical support of the

anatomical organization but it also plays a crucial role in the photosynthesis efficiency [4, 5] and in the consumption of water. Furthermore, the capillary branching of the veins in the leaf allows better cooling [6] with potential benefits for the photosynthesis performance [7]. Recent studies show that the vein density per unit area [8] and the thickness of the mesophyll [9] may be involved in the efficiency of hydraulic performance. A decreasing hydraulic functionality, due to water stress or to a limited vein network density, can involve a loss of production. The leaf water potential measurement, defined as the measure of the free energy per unit volume of water ( $J m^{-3}$ ) [10], explains the level of plant drought stress. The first water potential measurement came in 1960 with two basic instruments: the thermocouple psychrometer and the Scholander pressure chamber. Leaf water potential

\*Correspondence: [mario.pagano@crea.gov.it](mailto:mario.pagano@crea.gov.it)

<sup>†</sup>Lorenzo Baldacci and Mario Pagano contributed equally to this work

<sup>2</sup> Consiglio per la ricerca in agricoltura e l'analisi dell'economia agraria, Centro di ricerca per la Viticoltura e l'Enologia, Viale Santa Margherita 80, 52100 Arezzo, Italy

Full list of author information is available at the end of the article

measured with the Scholander pressure bomb [11] is considered the reference method by plant physiologists. However, this device needs a destructive sampling of the leaf and presents different operating limits: it requires a cylinder with a propellant of nitrogen (or compressed air), cumbersome instrumentation, long operating times and the measurements cannot be automated. The thermocouple psychrometer, instead, is based on the principle that the relative vapour pressure of a solution or piece of plant material is related to its water potential. The requirement of tight temperature control restricted the use of uncompensated thermocouple psychrometers in field studies to situations where good laboratory facilities were at hand. The water content of plants is another basic parameter which describes the plant water deficit and is commonly determined by weighing the material immediately after sampling, drying at 105 °C, and reweighing 24 h later; a process which is destructive, time-consuming and hard to be automated.

A growing attention in the scientific community has been directed to terahertz spectroscopic techniques, mostly time domain spectroscopy or confocal microscopy [12], as a non-invasive tool for measuring leaf water content [13, 14] and related quantities such as drought stress [15, 16] and dehydration kinetics [17]. The potential of THz absorption measurements was also demonstrated in the study of the hydration of biomolecules [18–20] and ions [21–24]. The terahertz spectral region is particularly promising in this branch of studies: thanks to the large absorption coefficient of water [25], opposite to the relatively small absorption coefficient of the leaf dry matter [13] terahertz techniques are more sensitive to changes in water content than near infrared and microwave techniques, because they suffer less disturbances from changes in concentration of soluble substances, such as inorganic salts [26]. Terahertz techniques have to face the major challenge of the translation from lab tables to the field. The measurement method must be thought of for non-ideal working conditions, hence robust and reliable, in addition to non-invasive [27].

In this work, we report on a method for measuring the leaf wet mass using a terahertz quantum cascade laser [28] (THz QCL) and a camera. This method is based on a linear law which relates the leaf wet mass to the product between its optical depth and projected area. We compared this new method with the one based on the sole terahertz transmission, by studying six plants of *Vitis vinifera* L. (cv “Colorino”). A linear regression model was employed to fit the data obtained from the two methods. In the first case we had the sole optical depth as function of the leaf wet mass, and the least square fit of the data set produced an adjusted coefficient of determination of 0.31. With the new method instead, the linear regression model was adopted

to fit the product between the leaf optical depth and the leaf projective area, as function of the leaf wet mass. In this case, the least square fit of the dataset has a coefficient of determination of 0.95, which means that the new method is reliable also when leaves come from different plants.

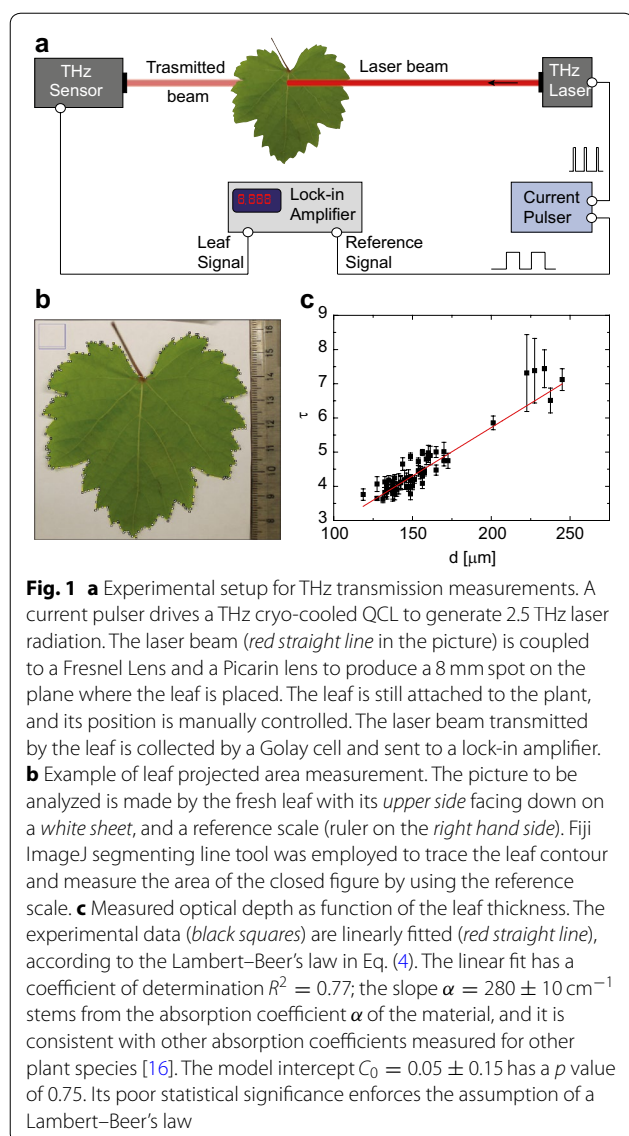
## Methods

### Plant preparation

All the experiments were performed in September 2015 on 2 year old vines. Six plants were pruned as a single-cordon and grafted onto SO4 (*V. berlandieri* × *V. riparia*) rootstock. *Vitis vinifera* L. (cv “Colorino”) were used for the trials. The plants were arranged to 2 L pots filled with a peat:sand mix (2:1). The vines were acclimated to the same environmental condition (24 °C; 45.5% of relative humidity; approximately 660  $\mu\text{mol m}^{-2} \text{s}^{-1}$  P.A.R.) inside the laboratory of the Department of physics at the University of Pisa, Italy. The measurements were performed under the same environmental conditions. Photon Flux measurements were conducted using em50 data logger (Decagon Devices, Inc.) equipped with a calibrated QSO-S PAR Photon Flux sensor. The environmental conditions, temperature and humidity, were measured with a calibrated usb temperature and humidity data logger (model IMD 100, Imaginationtronix Inc.). During the experiments, the photoperiod was 13 h 15 min day and 10 h 45 min night. For each of six plants all leaves fully extended and developed were sampled from the main shoot and, according to Kapos [29], the water content of leaves was determined by weighing the leaves immediately after sampling, drying at 105 °C, and reweighing 24 h later.

### Measurement setup

Leaf optical depths were measured by means of a simple transmission setup, like the one sketched in Fig. 1a. THz laser radiation produced by a THz QCL is shined onto the leaf. The fraction of light passing through the leaf tissues is then collected by a THz detector. The ratio between the total incident power and the transmitted one gives the experimental optical transmission data. The optical source was a THz QCL emitting at frequencies around 2.5 THz, cryo-cooled down to 30 K and driven by a current pulser. For each leaf, we measured its transmittance and thickness; then, right after detachment, leaf fresh mass and projective area were measured. In order to sample most of the leaf structure, the transmittance data were sampled over four different regions with a diameter of 8 mm: one from the petiolar sinus to the first bifurcation; one on the first order vase in the distal part; two on the lateral lobes, left and right. The regions are loosely defined in order to assess the robustness of the measurement procedure when different leaves are measured. The readout signal is measured by a Stanford



SR830 lock-in amplifier synchronized with the QCL current supply. To further suppress unwanted background and residual scattered radiation on the detector, a black screen with a 8 mm hole was placed behind the leaf sampling region. The black screen was made of an aluminum plate with a rough surface. In order to choose the hole width, a lever iris was placed along the optical path (the aluminum plate was removed) and the signal recorded by the detector was measured with increasing iris apertures, until the recorded signal did not change its least significant digit with respect to the case without the iris. During the transmission measurement the sample was held by hand. At the cost of some precision, the hand offers many translational and rotational degrees of freedom, enabling hardly reachable leaves to be placed in

the optical path. For each leaf the average optical depth was calculated starting from the transmittance data, by averaging over the four samples. The leaf thickness  $d_j$  was measured with a contact caliper by averaging over four 6 mm diameter regions, selected with the same criteria as the regions for the transmission measurement. Note that the thickness was measured over a region without major veins; in this way the thickness is underestimated by a factor 5–10% according to the literature [30]. The plant material was then detached and weighted to acquire the leaf fresh mass. Each projective area was measured immediately after weighting, with a procedure explained in Fig. 1b. The leaf was placed with its lower side facing up onto a white paper sheet with a scale reference on a side, and photographed. Its projective area was measured using Fiji ImageJ segmented line tool on the image collected [31]. Finally the leaf was dried for 24 h at a temperature of 105 °C and weighted to acquire its dry mass.

## Results

The main scope of our work is to find a relation between the leaf optical properties at THz frequencies and the leaf water content, which is reproducible for different plants of the same variety. We examined six plants of *Vitis vinifera* L. (cv “Colorino”) by measuring 58 leaves, chosen according to the Plant Preparation Section. The optical transmittance was sampled over four regions for each leaf, according to the Measurement setup Section. Given the  $j$ -th leaf, the optical transmittance of the  $k$ -th sample region is defined as the ratio between the laser beam intensity transmitted by the leaf to the detector,  $S_{j,k}$ , and the incident one,  $I_j$ :

$$T_{j,k} = \frac{S_{j,k}}{I_j}. \quad (1)$$

In order to perform statistical data analysis, for each leaf we calculate its average experimental optical depth  $\tau_{j,k}$ , defined by the Lambert–Beer’s law [32]

$$T_{j,k} = \exp[-\tau_{j,k}], \quad (2)$$

therefore  $\tau_{j,k}$  accounts for material losses. The average optical depth  $\tau_j$  can be calculated as

$$\tau_j = \frac{1}{4} \sum_{k=1}^4 \tau_{j,k}. \quad (3)$$

Within an effective medium approximation [33, 34],  $\tau_j$  is proportional to the effective leaf absorption coefficient  $\alpha_j$  and the leaf average thickness  $d_j$ :

$$\tau_j = \alpha_j d_j. \quad (4)$$

If all the leaves had the same distribution of water, air, and dry materials, their  $\alpha_j$  should be the same. In Fig. 1c

all the measured  $\tau_j$  are plotted against  $d_j$ , each leaf contributing with one point. The red straight line reports the linear best fit, resulting from a two parameter linear regression in which data are statistically weighted with the inverse of their variances, to account for heteroscedasticity. We found that our linear regression has a coefficient of determination of  $R^2 = 0.77$ , which means it is able to explain 77% of the overall  $\tau_j$  fluctuations around their mean value; the resulting effective absorption coefficient  $\alpha = 280 \pm 10 \text{ cm}^{-1}$  is similar to the ones found for other species (for example, measured *Coffea Arabica* effective absorption coefficient is  $\alpha \simeq 250 \text{ cm}^{-1}$  at a frequency of 1.8 THz [16]). Also the high  $p$  value related to the intercept parameter ( $C_0$  in Fig. 1c) confirms the consistency of the assumed Lambert–Beer’s law. It is worth to point out that we chose not to report the  $p$  value of those parameters having  $p$  value smaller than  $10^{-10}$ .

### Leaf water content and optical depth

Trying to extract the leaf water mass from global optical depth is not trivial, because air, water and dry materials might be combined in different fractions and give approximately the same absorption coefficient. This concept is graphically explained in Fig. 2a, where the experimental  $\tau$  has been plotted as function of the experimental leaf water mass  $M_W$ , which was measured for each leaf according to the Measurement Setup section. In this case the linear slope is statistically different from 0 with  $p$  value of  $3.8e - 6$ , but the linear regression

explains only 31% of the total data fluctuations. Better effective medium models could improve the predictions on leaf water mass. Recently, Landau–Lifshitz–Looyenga model has been successfully employed on *Coffea Arabica* and *Hordeum Vulgare* plants [13, 16], at the expense of new variables to be measured, such as the leaf dry material refractive index, which requires the leaf to be dehydrated and pelletized. In this work we found a simpler model to enhance the description of the experimental data, by combining  $M_W$  with the leaf projective area  $A$ . If the optical depth is dominated by water absorption, Eq. (4) may be rewritten as:

$$\tau = \alpha_{\text{eff}} d_W, \quad (5)$$

where  $\alpha_{\text{eff}}$  is the effective absorption coefficient and  $d_W = V_W/A$  is the effective water thickness inside the leaf, expressed as the ratio between the volume of water inside the leaf and the leaf projective area. Water volume may be safely expressed as function of the water mass  $M_W$ , because water density is known and can be approximated to  $\rho_W = 1000 \text{ mg cm}^{-3}$ ; Eq. (5) then becomes

$$\tau = \mathbb{K} \frac{M_W}{A}, \quad (6)$$

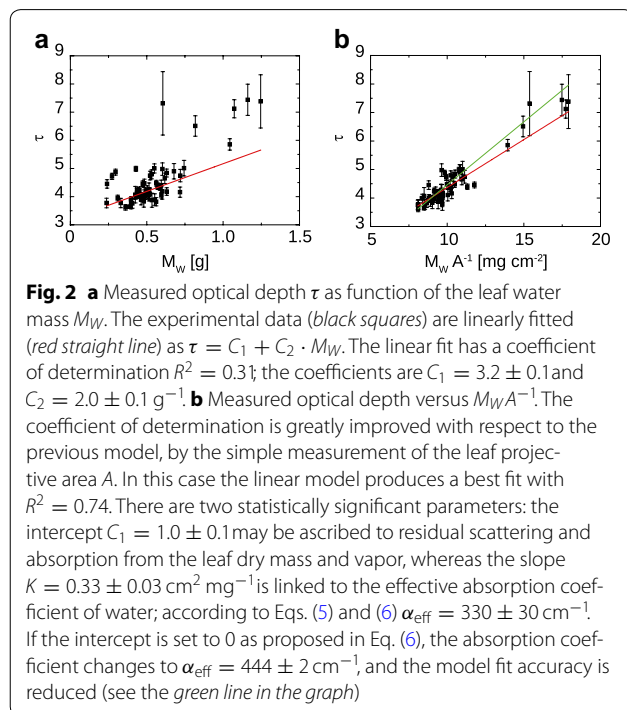
where  $\mathbb{K} = \alpha_{\text{eff}}/\rho_W$ . Looking at Fig. 2b, we see the linear regression of  $\tau$  as function of  $M_W \cdot A^{-1}$ . In this case the best fit of linear regression (red line) returns  $\mathbb{K} = 0.33 \pm 0.03 \text{ cm}^2 \text{ mg}^{-1}$ , which means an absorption coefficient  $\alpha_{\text{eff}} = 330 \pm 30 \text{ cm}^{-1}$ , but also an intercept  $C_1 = 1.0 \pm 0.1$ , which is statistically different from 0 with very small  $p$  value; this result entails a non-negligible contribution to losses from dry mass and/or vapor absorption, and from scattering due to the heterogeneity of the leaf tissues. The coefficient of determination is greatly improved with respect to the sole use of  $M_W$ , with  $R^2 = 0.74$ , which means that optical depth data describe almost 75% of the  $M_W \cdot A^{-1}$  data fluctuations. If the intercept is set to 0, from the linear fit (green line in Fig. 2b) we find  $\alpha_{\text{eff}} = 444 \pm 2 \text{ cm}^{-1}$ ; in this case the accuracy of the model is slightly reduced, because the residual sum of squares  $\sum_{j=1}^{58} (\tau_j - \tau_j(\text{model}))$  increases by  $\sim 29\%$ . By adding a term which is inversely proportional to  $A$ , Eq. (6) is transformed into

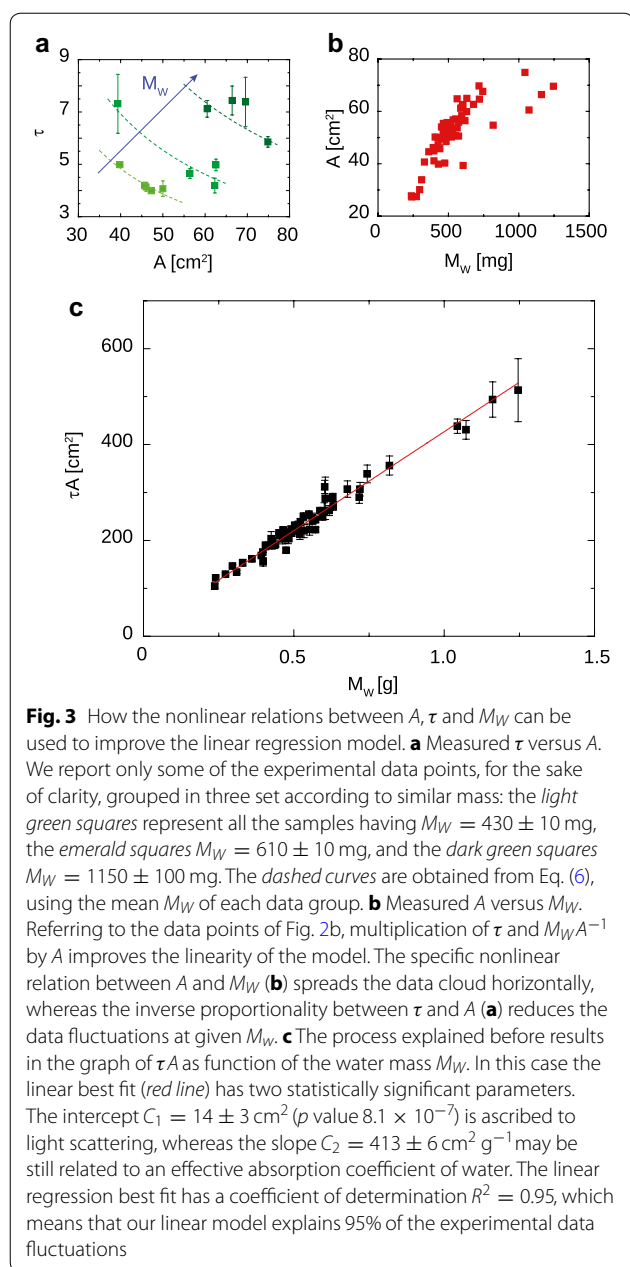
$$\tau = \frac{C_1}{A} + C_2 \frac{M_W}{A}, \quad (7)$$

where  $C_1$  and  $C_2$  are constant coefficients. By moving  $A$  on the left hand side of the equation we obtain a linear relation

$$\tau A = C_1 + C_2 M_W. \quad (8)$$

In Fig. 3c we report the linear regression best fit of the experimental data  $\tau_j A_j$  as function of the leaf





water mass data  $M_j$ . We found that the variable  $\tau A$  describes the water mass experimental data with 95% of accuracy, and both coefficients have statistically relevant values,  $C_1 = 14 \pm 3 \text{ cm}^2$  ( $p$  value  $8.1 \times 10^{-7}$ ) and  $C_2 = 413 \pm 6 \text{ cm}^2 \text{ g}^{-1}$ . The inverse proportionality with  $A$  of the term  $C_1 A^{-1}$  in Eq. (7) could be ascribed to the nonlinear correlation between the leaf projective area and the water mass, as shown in Fig. 3a (lower graph): the larger is  $M_W$ , the slower is the increase of  $A$ , and the contribution of bulk absorption becomes more important.

## Discussions

The reason why the use of Eq. (8) improves the linear regression, as shown in Fig. 3c, can be found inside the nonlinear relation between  $A$ ,  $M_W$ , and  $\tau$ , and it is graphically explained in Fig. 3, panels a and b. Here we report the two graphs of  $\tau$  versus  $A$  (panel a) and  $A$  versus  $M_W$  (panel b). Multiplication by  $A$  on both sides of Eq. (7) produces two synergical actions. It has a horizontal action, because lower values of  $A$  grow more steeply with  $M_W$  than higher values, as shown in Fig. 3b; this effect tends to horizontally elongate the data cloud in Fig. 2b. There is also a vertical action, which can be explained looking at Fig. 3a. Here we reported three groups of data points, based on similarity of  $M_W$ . The first group (light green squares) has  $M_W = 430 \pm 10$  mg, the second (emerald squares)  $M_W = 610 \pm 10$  mg, the third (dark green squares)  $M_W = 1150 \pm 100$  mg. The dashed lines indicate the curves found using Eq. (6) and the mean  $M_W$  of each group. Since the curves reasonably fit the data points, we may consider  $A$  and  $\tau$  to be inversely proportional; consequently, multiplication of  $\tau$  by  $A$  reduces the data fluctuations at given  $M_W$ . The good agreement between the model Eq. (8) and the experimental data tells us that the model is robust enough to describe different plants of the same variety. During our experiment, leaves were detached from the plants after measuring the THz transmission, in order to perform the gravimetric measurements. Our treatment provided the leaf projective area by simply placing the leaf onto a white page with a scale bar on it. This method can of course be improved by placing a scalebar directly in the THz transmission setup. With this simple adaptation, the measurement of both the optical depth and the leaf projective area would become telemetric, thus exploitable for non-invasive measurements. Two other important points to take care of are the cryogenic temperature of the THz source and the leaf temperature. The cryo-cooler employed in this work mounts a Gifford-McMahon motor, which is free from cryogenic liquids such as liquid helium or liquid nitrogen; despite that, its size and weight would be impractical for in field measurements, requiring relatively large water-cooled compressors. This issue can be overcome by using low-current, high-efficiency THz QCLs [35]: they can be operated on board of compact, self-contained Stirling cryo-coolers, that necessitate only of limited electrical power ( $\sim 10$  W) and air cooling. Temperature is also an important factor in determining the water absorption coefficient, whose variation is of the order of 10% ranging from 25 to 35 °C. In this case a model describing how the dielectric permittivity of water changes with temperature is discussed in [36]: after the absorption coefficient is defined as function of the temperature, a conversion table can be arranged in

order to normalize the in-field data with respect to the leaf temperature conditions, which could be probed for example by using an infrared thermometer [37]. Finally, our results unlock an interesting question about the measurements. The confidence of our linear fit depends on the specific relation between leaf water mass and leaf projective area. This relation could change with the plant species, and it will be the subject of future theoretical and experimental studies. The main result of this work can now be summarized: using Eq. (8) we are able to measure the water mass inside a grapevine leaf by means of two potentially telemetric measurements, which are fast, non-invasive, and reliable.

## Conclusions

In this work, we developed a new method for measuring the leaf water mass using a THz QCL, based on a leaf statistical sampling and a linear equation which relates the leaf water mass to the product between the optical depth and the leaf projected area. The results are in very good agreement with the model proposed here, proving the robustness and reliability of our new technique, which is under patent filing (application no. 102016000106179). Our method can be employed when plant averaged or cumulative data are required. For example, the canopy water mass can be combined with other plant parameters such as the biomass fresh and dry weight or the grain yield, and used as diagnostic indicators for cultivars under drought stress [38]. In future experiments, further calibration curves will be performed on other plant genotypes in order to prove our law or find other ones, whereas new relations between the shape of the scaling law and different plant behaviours could be highlighted, e.g. when preserving the water status during drought stress. By combining our technique with a gas exchange analyser, experiments can be carried out monitoring plant physiological aspects such as stomatal conductance and water potential directly in the laboratory or in the field. Furthermore, the different vein architecture among polyhedral leaves may be related to different management of water demand within the hydraulic network.

## Authors' contributions

LB prepared the terahertz transmission setup, the experimental protocol, and performed the data analysis; MP prepared the plant material and the experimental protocol; LM prepared the terahertz transmission setup and the experimental protocol. MP, LB and LM performed the measurements. AT performed the data analysis and supervised the work. GC prepared the experimental setup. PS and AT supervised the work. All authors contributed to writing the article. All authors read and approved the final manuscript.

## Author details

<sup>1</sup> NEST, CNR Istituto Nanoscienze and Scuola Normale Superiore, Piazza San Silvestro 12, 56127 Pisa, Italy. <sup>2</sup> Consiglio per la ricerca in agricoltura e l'analisi dell'economia agraria, Centro di ricerca per la Viticoltura e l'Enologia, Viale Santa Margherita 80, 52100 Arezzo, Italy. <sup>3</sup> Dipartimento di Fisica, Università di Pisa, Largo Pontecorvo 3, 56127 Pisa, Italy. <sup>4</sup> NEST, CNR Istituto Nanoscienze

and Dipartimento di Fisica, Università di Pisa, Largo Pontecorvo 3, 56127 Pisa, Italy.

## Acknowledgements

Not applicable.

## Competing interests

The authors declare that they have no competing interests.

## Availability of data and materials

All data generated or analysed during this study are included in this published article.

## Funding

Funding information is not applicable.

## Use of plant material

We did not use any genetically modified material nor opiaceous. Our plant treatments were not subject to any particular guideline or legislation.

## Publisher's Note

Springer Nature remains neutral with regard to jurisdictional claims in published maps and institutional affiliations.

Received: 7 December 2016 Accepted: 6 June 2017

Published online: 17 June 2017

## References

- Fischer G, Tubiello FN, Van Velthuisen H, Wiberg DA. Climate change impacts on irrigation water requirements: effects of mitigation, 1990–2080. *Technol Forecast Soc Change*. 2007;74(7):1083–107.
- Schulze E-D, Robichaux R, Grace J, Rundel P, Ehleringer J. Plant water balance. *Bioscience*. 1987;37:30–7.
- Brodribb TJ, Feild TS, Jordan GJ. Leaf maximum photosynthetic rate and venation are linked by hydraulics. *Plant Physiol*. 2007;144(4):1890–8.
- Price CA, Symonova O, Mileyko Y, Hilley T, Weitz JS. Leaf extraction and analysis framework graphical user interface: segmenting and analyzing the structure of leaf veins and areoles. *Plant Physiol*. 2011;155(1):236–45.
- Pagano M, Corona P, Storchi P. Image analysis of the leaf vascular network: physiological considerations. *Photosynthetica*. 2016;54:567–71. doi:10.1007/s11099-016-0238-2.
- Pagano M, Storchi P. Leaf vein density: a possible role as cooling system. *J Life Sci*. 2015;9:299–303.
- Chaves MM, Pereira JS, Maroco J, Rodrigues ML, Ricardo CPP, Osório ML, Carvalho I, Faria T, Pinheiro C. How plants cope with water stress in the field. *Photosynthesis and growth*. *Ann Bot*. 2002;89(7):907–16.
- Sack L, Frolke K. Leaf structural diversity is related to hydraulic capacity in tropical rain forest trees. *Ecology*. 2006;87(2):483–91.
- Aasamaa K, Söber A, Rahi M. Leaf anatomical characteristics associated with shoot hydraulic conductance, stomatal conductance and stomatal sensitivity to changes of leaf water status in temperate deciduous trees. *Funct Plant Biol*. 2001;28(8):765–74.
- Taiz L, Zeiger E. *Plant physiology*. 5th ed. Sunderland: Sinauer Assoc; 2010.
- Scholander PF, Bradstreet ED, Hemmingsen E, Hammel H. Sap pressure in vascular plants negative hydrostatic pressure can be measured in plants. *Science*. 1965;148(3668):339–46.
- Jepsen PU, Cooke DG, Koch M. Terahertz spectroscopy and imaging—modern techniques and applications. *Laser Photon Rev*. 2011;5(1):124–66.
- Gente R, Koch M. Monitoring leaf water content with thz and sub-thz waves. *Plant Methods*. 2015;11(1):15.
- de Cumis US, Xu J-H, Masini L, Degl'Innocenti R, Pingue P, Beltram F, Tredicucci A, Vitiello MS, Benedetti PA, Beere HE, et al. Terahertz confocal microscopy with a quantum cascade laser source. *Opt. Express*. 2012;20(20):21924–31.
- Born N, Behringer D, Liepelt S, Beyer S, Schwerdtfeger M, Ziegenhagen B, Koch M. Monitoring plant drought stress response using terahertz time-domain spectroscopy. *Plant Physiol*. 2014;164(4):1571–7.

16. Jördens C, Scheller M, Breitenstein B, Selmar D, Koch M. Evaluation of leaf water status by means of permittivity at terahertz frequencies. *J Biol Phys*. 2009;35(3):255–64.
17. Castro-Camus E, Palomar M, Covarrubias A. Leaf water dynamics of *Arabidopsis thaliana* monitored in-vivo using terahertz time-domain spectroscopy. *Sci Rep*. 2013;3:2910.
18. Heugen U, Schwaab G, Bründermann E, Heyden M, Yu X, Leitner D, Havenith M. Solute-induced retardation of water dynamics probed directly by terahertz spectroscopy. *Proc Natl Acad Sci*. 2006;103(33):12301–6.
19. Arikawa T, Nagai M, Tanaka K. Characterizing hydration state in solution using terahertz time-domain attenuated total reflection spectroscopy. *Chem Phys Lett*. 2008;457(1):12–7.
20. Grossman M, Born B, Heyden M, Tworowski D, Fields GB, Sagi I, Havenith M. Correlated structural kinetics and retarded solvent dynamics at the metalloprotease active site. *Nat Struct Mol Biol*. 2011;18(10):1102–8.
21. Schmidt DA, Birer O, Funkner S, Born BP, Gnanasekaran R, Schwaab GW, Leitner DM, Havenith M. Rattling in the cage: ions as probes of sub-picosecond water network dynamics. *J Am Chem Soc*. 2009;131(51):18512–7.
22. Heisler IA, Meech SR. Low-frequency modes of aqueous alkali halide solutions: glimpsing the hydrogen bonding vibration. *Science*. 2010;327(5967):857–60.
23. Tielrooij K, Van Der Post S, Hunger J, Bonn M, Bakker H. Anisotropic water reorientation around ions. *J Phys Chem B*. 2011;115(43):12638–47.
24. Funkner S, Niehues G, Schmidt DA, Heyden M, Schwaab G, Callahan KM, Tobias DJ, Havenith M. Watching the low-frequency motions in aqueous salt solutions: the terahertz vibrational signatures of hydrated ions. *J Am Chem Soc*. 2011;134(2):1030–5.
25. Hale GM, Querry MR. Optical constants of water in the 200-nm to 200- $\mu$ m wavelength region. *Appl Opt*. 1973;12(3):555–63.
26. Ulaby FT, Jedlicka R. Microwave dielectric properties of plant materials. *IEEE Trans Geosci Remote Sens*. 1984;4:406–15.
27. Fiorani F, Schurr U. Future scenarios for plant phenotyping. *Annu Rev Plant Biol*. 2013;64:267–91.
28. Köhler R, Tredicucci A, Beltram F, Beere HE, Linfield EH, Davies AG, Ritchie DA, Iotti RC, Rossi F. Terahertz semiconductor-heterostructure laser. *Nature*. 2002;417(6885):156–9.
29. Kapos V. Effects of isolation on the water status of forest patches in the Brazilian Amazon. *J Trop Ecol*. 1989;5(02):173–85.
30. Sack L, Scoffoni C, McKown AD, Frole K, Rawls M, Havran JC, Tran H, Tran T. Developmentally based scaling of leaf venation architecture explains global ecological patterns. *Nat Commun*. 2012;3:837.
31. Schindelin J, Arganda-Carreras I, Frise E, Kaynig V, Longair M, Pietzsch T, Preibisch S, Rueden C, Saalfeld S, Schmid B, et al. Fiji: an open-source platform for biological-image analysis. *Nat Methods*. 2012;9(7):676–82.
32. Bhatt M, Ayyalomasayajula KR, Yalavarthy PK. Generalized Beer–Lambert model for near-infrared light propagation in thick biological tissues. *J Biomed Opt*. 2016;21(7):076012.
33. Scheller M, Jansen C, Koch M, et al. Applications of effective medium theories in the terahertz regime. London: INTECH Open Access Publisher; 2010.
34. Kocsis L, Herman P, Eke A. The modified Beer–Lambert law revisited. *Phys Med Biol*. 2006;51(5):91.
35. Amanti MI, Scalari G, Castellano F, Beck M, Faist J. Low divergence terahertz photonic-wire laser. *Opt Express*. 2010;18(6):6390–5.
36. Ellison W. Permittivity of pure water, at standard atmospheric pressure, over the frequency range 0–25 THz and the temperature range 0–100 °C. *J Phys Chem Ref Data*. 2007;36(1):1–18.
37. Winterhalter L, Mistele B, Jampatong S, Schmidhalter U. High throughput phenotyping of canopy water mass and canopy temperature in well-watered and drought stressed tropical maize hybrids in the vegetative stage. *Eur J Agron*. 2011;35(1):22–32.
38. Elsayed S, Darwish W. Hyperspectral remote sensing to assess the water status, biomass, and yield of maize cultivars under salinity and water stress. *Bragantia*. 2017;76(1):62–72.

Submit your next manuscript to BioMed Central and we will help you at every step:

- We accept pre-submission inquiries
- Our selector tool helps you to find the most relevant journal
- We provide round the clock customer support
- Convenient online submission
- Thorough peer review
- Inclusion in PubMed and all major indexing services
- Maximum visibility for your research

Submit your manuscript at  
[www.biomedcentral.com/submit](http://www.biomedcentral.com/submit)

